Electroosmotic Flow in a Tube or Channel at Non-Negligible Zeta Potentials

Stewart K. Griffiths and Robert H. Nilson
Sandia National Laboratories
Livermore, California 94551-0969

ABSTRACT

Numerical methods based on a shooting technique are employed to determine the electric potential and fluid velocity in a tube and channel when the zeta potential is not small. In addition, new analytical solutions are presented for the fluid velocity in the extreme of a small Debye layer thickness. Asymptotic expressions for these results are provided for the limits of small and large zeta potentials. We find that increasing values of the wall potential always increase the mean fluid speed and yield a velocity profile having a more uniform speed near the center of the tube or channel.

Keywords: electroosmotic, electrokinetic, flow

1 INTRODUCTION

Electroosmotic flows [1,2] offer two important benefits over pressure-driven flows for transport processes in microchannel devices. First, fluid speeds in electroosmotic flows are independent of the transverse dimension of the tube or channel over a wide range of conditions, making this technique for driving fluid motion extensible to extremely small physical scales. Second, the profile of the fluid velocity across a tube or channel is essentially flat, again over a very wide range of conditions. The benefit of this is that solute samples may be transported over long ranges with little dispersion due to nonuniform fluid speeds.

Fluid velocities in electroosmotic flow in tubes and channels are well known for the special case of a negligible normalized zeta potential at the tube or channel wall. In both geometries, analytical solutions to the equations governing the electric potential and fluid velocity have been obtained in closed form. These solutions apply to all values of the normalized Debye layer thickness. Such broad solutions have not been obtained for cases in which the zeta potential is not small.

In the present study, analytical and numerical methods are employed to determine the electric potential and fluid velocities for electroosmotic flow in a tube and channel when the zeta potential is not small. Numerical results are presented for a wide range of values of the normalized Debye layer thickness and the normalized zeta potential. In addition, new analytical solutions are presented for the mean fluid speed and local fluid velocity in the extreme of a small Debye layer thickness. These are valid for all values of the zeta potential.

2 GOVERNING EQUATIONS

Here we consider two-dimensional planar or axisymmetric flow in a tube or channel. The flow is assumed incompressible and transport properties are assumed constant. Under these restrictions, and further assuming that the flow is steady and that inertial effects are small, the momentum equation may be written as

$$\mu \nabla^2 \mathbf{u} = \rho_e \nabla \phi \tag{1}$$

where μ is the fluid viscosity, ρ_e is the net local charge density, and ϕ is the local electric potential. Finally, for a dielectric constant, ϵ, that does not vary with position, the Poisson equation governing the electric field is

$$\epsilon \, \nabla^2 \phi = -\rho_e \tag{2}$$

and the local charge density may be related to the electric potential through the Boltzmann distribution given by $\rho_e = -2Fzc_e \sinh(zF\phi/RT)$, where F is the Faraday constant, z is the ion charge number, c_e is the bulk fluid ion concentration, R is the universal gas constant, and T is the temperature.

We now introduce new normalized dependent variables, taken as $\mathbf{u}^* = \mathbf{u}/U$ and $\phi^* = \phi/\zeta$, where U is the mean axial fluid speed averaged across the tube or channel, and ζ is the electric potential at the tube or channel wall. The new independent variables are $x^* = x/a$ and $y^* = y/a$, where x and y are the axial and transverse coordinates, and a is the tube radius or channel half-height. This normalization leads to two new parameters, the normalized Debye length,

$$\lambda^{*2} = \left(\frac{\lambda}{a}\right)^2 = \frac{\epsilon RT}{2F^2 z^2 c_e a^2} \tag{3}$$

and the normalized wall potential, $\zeta^* = zF\zeta/RT$. The normalization additionally introduces one dimensionless unknown constant, $\beta = -\mu U/\epsilon \zeta E_x$. This is the mean axial fluid speed normalized by the Helmholtz-Smoluchowski speed for flow past a charged surface.

Introducing these normalized variables into the primitive governing equations and rearranging slightly yields

$$\beta \, \nabla^2 \mathbf{u}^* = -\nabla^2 \phi^* \, \mathbf{E}^* \tag{4}$$

$$\lambda^{*2} \, \nabla^2 \phi^* = \frac{1}{\zeta^*} \sinh\left(\zeta^* \phi^*\right) \tag{5}$$

The new dependent variable, $\mathbf{E}^* = -\nabla\phi/E_x$ is the electric field vector normalized by the applied axial electric

field, E_x. Boundary conditions for the normalized fluid velocities are $du^*/dy^*=0$ at $y^*=0$ and $u^*=0$ at $y^*=1$. Those for the electric potential are $\partial\phi^*/\partial y^*=0$ at $y^*=0$ and $\phi^*=1$ at $y^*=1$.

Recognizing that the incompressible flow in a long tube or channel must be one dimensional, and that the radial component of the fluid velocity is therefore everywhere zero, and further recognizing that the second derivative of the electric potential in the axial direction is small compared to that in the transverse direction, we see that the normalized fluid velocity can be expressed directly in terms of the normalized electric potential as

$$u^* = \frac{1-\phi^*}{\beta} \tag{6}$$

Integrating this result across the tube or channel and equating the result to unity then yields an explicit expression for the normalized mean fluid speed

$$\beta = -\frac{\mu U}{\epsilon \zeta E_x} = (n+1)\int_0^1 (1-\phi^*)\, y^{*n} dy^* \tag{7}$$

The parameter n in Eq. (7) describes either the planar or axisymmetric geometries by taking $n=0$ or 1, respectively.

3 METHOD OF SOLUTION

Equation (5) governing the electric potential possesses closed-form solutions satisfying all specified boundary conditions only for cases in which the normalized zeta potential, ζ^*, is vanishingly small. In general, Eq. (5) and the dependent equations describing the fluid velocity and transverse variation of the solute concentration must be solved numerically. For this we employ a very accurate shooting technique based on the following procedure.

Given values of λ^* and ζ^*, Eq. (5) is first integrated from $y^*=0$ to $y^*=1$ using the boundary condition $\phi^{*\prime}(0)=0$ and an initial guess for $\phi^*(0)$. The resulting value of $\phi^*(1)$ does not necessarily satisfy the required boundary condition $\phi^*(1)=1$, so an improved value of $\phi^*(0)$ is computed based on the discrepancy between the observed and required boundary values. This process is repeated to convergence, each time using the improved estimate of $\phi^*(0)$ to begin the integration. These integrations are performed using a double-precision routine, DDERKF [3], with specified relative and absolute error tolerances of 10^{-12} and 10^{-20}, respectively. New values of $\phi^*(0)$ are computed automatically using the nonlinear algebraic equation solver DNSQE [3].

Once the electric potential is known, the corresponding value of β is computed from Eq. (7). The required quadrature is performed by integrating Eqs. (5) and (7) together as a coupled pair, using the correct value of $\phi^*(0)$ previously determined. From Eq. (6), the velocity profile is then known.

The shooting procedure described above works well when λ^* is greater than about 10^{-3}. For smaller values, the shooting target becomes difficult to hit since very small changes in $\phi^*(0)$ then yield large changes in $\phi^*(1)$. Because of this, an alternate method is employed when λ^* is very small. When λ^* is small, the electric potential varies only in a region close to the tube or channel wall. The boundary condition $\phi^{*\prime}(0)=0$ becomes nearly superfluous in this limit, and the electric potential can be well approximated by [4]

$$\phi^* \sim \frac{4}{\zeta^*}\operatorname{arctanh}\left[e^{(y^*-1)/\lambda^*}\tanh\left(\frac{\zeta^*}{4}\right)\right] \tag{8}$$

as $\lambda^*\to 0$. This is an exact solution to Eq. (5) for all ζ^* and satisfies the boundary condition $\phi^*(1)=1$. It is approximate only in the sense that the condition $\phi^{*\prime}(0)=0$ is not satisfied exactly except in the limit $\lambda^*\to 0$. In practice, however, this solution is very accurate for all λ^* less than about 0.01. Shooting is thus unnecessary when λ^* is small, and the electric potential can be described instead by this closed-form result.

4 FLUID MOTION IN A TUBE

The computed normalized electric potential and axial fluid speed are shown in Fig. 1 for electroosmotic flow in a tube. These sample results are for $\lambda^*=0.3$ and a range of values of ζ^*. Here we see that increasing ζ^* is somewhat analogous to decreasing λ^*. In both cases, the electric potential and fluid velocity develop a steeper gradient near the tube wall, but then exhibit an increased region of nearly uniform values near the centerline.

Figure 2 shows computed values of the normalized mean fluid speed, β, for a wide range of values of λ^* and ζ^*. Here we see that increasing ζ^* always increases β. This is again because larger ζ^* yields an effectively smaller Debye layer thickness and so yields a normalized electric potential closer to zero over a broader portion of the tube cross-section. By Eq. (7), β is thus increased. We also see that β approaches unity as λ^* becomes small and falls as $1/\lambda^{*2}$ for all ζ^* as λ^* grows large.

In addition to numerical results like those of Figs. 1 and 2, we have obtained analytical solutions for the fluid velocity in the extremes of small and large λ^*. Such solutions serve to quantify the general observations above and further provide valuable benchmark results for testing more general finite-difference and finite-element methods. Recall from Eq. (6) that the local fluid speed under all conditions is given by $u^*=(1-\phi^*)/\beta$. Thus local axial fluid speeds, u^*, are uniquely determined by specifying only the normalized electric potential, ϕ^*, and the normalized mean axial fluid speed, β. These are given below in analytical form for small and large λ^*.

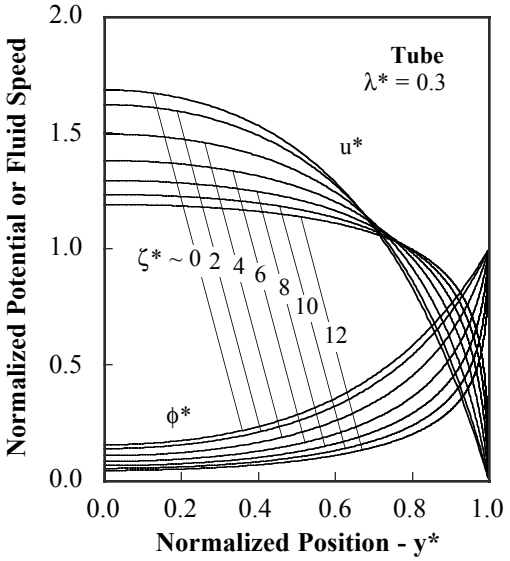

Figure 1. Normalized electric potential (ϕ^*) and normalized fluid speed (u^*) for electroosmotic flow in a tube at non-negligible zeta potentials.

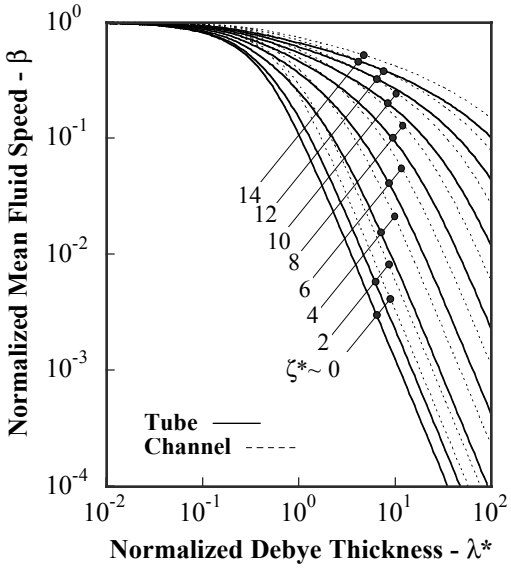

Figure 2. Normalized mean fluid speed for electroosmotic flow in a tube (solid) and channel (dashed) at non-negligible zeta potentials.

In the important practical limit of small λ^*, the electric potential is given by Eq. (8) and the corresponding normalized mean fluid speed is

$$\beta \sim 1 - \frac{4\lambda^*}{\zeta^*}\left[\mathrm{Li}_2(\xi) - \mathrm{Li}_2(-\xi)\right] \quad \text{as} \quad \lambda^* \to 0 \tag{9}$$

where $\xi = \tanh(\zeta^*/4)$ and $\mathrm{Li}_2(\xi)$ is the dilogarithm function,

$$\mathrm{Li}_2(\xi) = -\int_0^\xi \ln(1-s)\frac{ds}{s} = \sum_{k=1}^{\infty}\frac{\xi^k}{k^2} \tag{10}$$

This result, correct to order λ^*, was obtained by integrating Eq. (8) in accordance with Eq. (7) defining the normalized mean fluid speed. It agrees with the value of β computed numerically within 5% for all ζ^* when λ^* is less than 0.5; when λ^* is less than 0.2, the two agree within 1%.

The asymptotic behavior of Eq. (8) in the limit of small ζ^* is

$$\phi^* \sim e^{(y^*-1)/\lambda^*}\left(1 - \frac{\zeta^{*2}}{48}\left[1 - e^{2(y^*-1)/\lambda^*}\right]\right) \tag{11}$$

as $\lambda^* \to 0$ and $\zeta^* \to 0$. The corresponding normalized axial speed in this double limit is

$$\beta \sim 1 - 2\,\lambda^*\left(1 - \frac{\zeta^{*2}}{72}\right) \quad \text{as} \quad \lambda^* \to 0,\ \zeta^* \to 0 \tag{12}$$

This expression for β is consistent with our previous result [5] of $\beta = 1 - 2\lambda^* I_1(1/\lambda^*)/I_0(1/\lambda^*) \sim 1 - 2\lambda^*$ for the case of vanishingly small ζ^*. The values of $1-\beta$ computed using Eq. (12) agree with those of Eq. (9) within 3% for $\zeta^* \le 2$ and within 15% for $\zeta^* \le 4$. Note that the mean normalized fluid speed varies weakly with ζ^* when ζ^* is small. The term $\zeta^{*2}/72$ yields a correction to $1-\beta$ of only about 5% for $\zeta^* = 2$.

In the alternate extreme of large ζ^*, the asymptotic behavior of Eq. (8) is

$$\phi^* \sim -\frac{2}{\zeta^*}\ln\left[\mathrm{sech}^2\Big(\frac{y^*-1}{2\lambda^*}\Big)e^{-\zeta^*/2} - \tanh\Big(\frac{y^*-1}{2\lambda^*}\Big)\right] \tag{13}$$

as $\lambda^* \to 0$ and $\zeta^* \to \infty$. This yields a corresponding normalized mean fluid speed of

$$\beta \sim 1 - \lambda^*\frac{\pi^2}{\zeta^*} \quad \text{as} \quad \lambda^* \to 0,\ \zeta^* \to \infty \tag{14}$$

This expression for β can be obtained directly from Eq. (10) since $\xi \to 1$ as $\zeta^* \to \infty$ and $\mathrm{Li}_2(1) - \mathrm{Li}_2(-1) = \pi^2/4$. Values of $1-\beta$ computed using Eq. (14) agree with those of Eq. (11) within 3% for $\zeta^* \ge 10$, and within 1% for $\zeta^* \ge 14$.

5 FLUID MOTION IN A CHANNEL

Results paralleling those of Fig. 1 for a tube are shown for a channel in Fig. 3. Normalized mean fluid speeds for a channel appear in the previous Fig. 2 as dashed curves. These results are very similar to those for a tube, except that β for a channel is everywhere higher than that for a tube at the same λ^* and ζ^*.

In the limit $\lambda^* \to 0$, the electric potential given in Eq. (8) applies equally to a tube and a channel since the Debye layer thickness is then very small compared to the tube diameter or channel width. Despite this, the

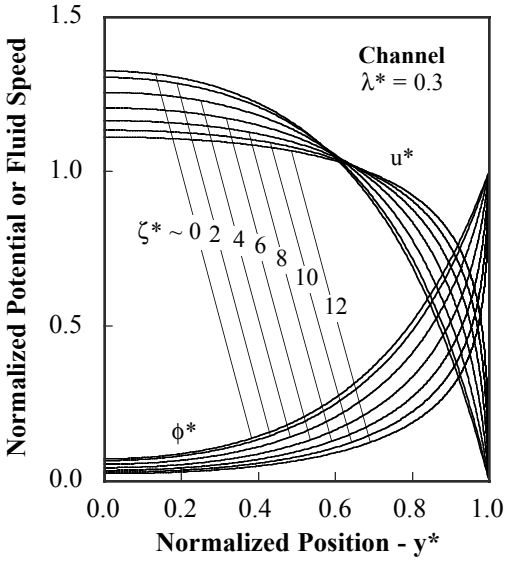

Figure 3. Normalized electric potential (ϕ^*) and normalized fluid velocity (u^*) for electroosmotic flow in a channel.

value of β differs between the two geometries owing to the difference in Eq. (7) for the two cases. For a channel, the normalized mean fluid speed for small λ^* is

$$\beta \sim 1 - \frac{2\lambda^*}{\zeta^*}\left[\mathrm{Li}_2(\xi) - \mathrm{Li}_2(-\xi)\right] \quad \text{as} \quad \lambda^* \to 0 \tag{15}$$

where again $\xi = \tanh(\zeta^*/4)$ and $\mathrm{Li}_2(\xi)$ is the dilogarithm function given by Eq. (10). As before, this result was obtained using the analytical expression for the electric potential given by Eq. (8). The accuracy and applicable range of this result are comparable to the parallel result for a tube, given by Eq. (9).

In the limit of small λ^* and small ζ^*, the electric potential in a channel is again the same as that in a tube and is given by Eq. (11). The corresponding asymptotic behavior of Eq. (15) in this small ζ^* limit is

$$\beta \sim 1 - \lambda^*\left(1 - \frac{\zeta^{*2}}{72}\right) \quad \text{as} \quad \lambda^* \to 0,\ \zeta^* \to 0 \tag{16}$$

This expression for a channel is again consistent with our previous solution $\beta = 1 - \lambda^* \tanh(1/\lambda^*) \sim 1 - \lambda^*$ for vanishing ζ^* [5]. The asymptotic behavior of Eq. (15) at large ζ^* is

$$\beta \sim 1 - \lambda^* \frac{\pi^2}{2\zeta^*} \quad \text{as} \quad \lambda^* \to 0,\ \zeta^* \to \infty \tag{17}$$

The corresponding potential in this limit is again given by Eq. (13), which applies to both the tube and channel geometries when λ^* is small. The accuracy and applicable range of Eqs. (13) and (14) are comparable to those of the corresponding results for a tube.

6 SUMMARY

We have examined the electroosmotic fluid motion in a tube and a channel for cases in which the zeta potential is not negligibly small. Using both numerical and analytical methods, the transverse variation of the electric potential and fluid speed were computed over a broad range of the normalized Debye layer thickness, λ^*, and the normalized zeta potential, ζ^*.

The numerical procedure used here is based on a shooting method. This procedure was checked against previously-published analytical and numerical solutions for both large and small values of the zeta potential [5,6,7]. In comparisons with analytical results for a negligible zeta potential, the two agree within a relative error of 10^{-6} for all values of the transverse position and values of λ^* between 10^{-3} and 10^3.

Analytical solutions were also obtained for the fluid velocity in a tube and channel in the asymptotic limits of small λ^*. The accuracy and applicable range of each solution is discussed, and expansions of the solutions for large and small ζ^* are provided.

ACKNOWLEDGMENT

This work was funded by a Sandia Phenomenological Modeling and Engineering Simulations LDRD. Sandia is operated by Sandia Corporation for the United States Department of Energy.

REFERENCES

[1] R. F. Probstein, *Physicochemical Hydrodynamics*, John Wiley & Sons, New York, NY (1995).

[2] C. L. Rice and R. Whitehead, "Electrokinetic Flow in a Narrow Cylindrical Capillary," *J. Phys. Chem.*, **69**, 4017, 1965.

[3] K. H. Haskell, W. H. Vandevender and E. L. Walton, "The SLATEC Mathematical Subprogram Library: SNL Implementation," SAND80-2992, Sandia National Laboratories, Albuquerque, NM, 1980.

[4] H. Poppe, A. Cifuentes and W. T. Kok, "Theoretical Description of the Influence of External Radial Fields on the Electroosmotic Flow in Capillary Electrophoresis," *Anal. Chem.*, **68**, 888, 1996.

[5] S. K. Griffiths and R. H. Nilson, "Hydrodynamic Dispersion of a Neutral Non-Reacting Solute in Electroosmotic Flow," *Anal. Chem.*, **71**, 5522, 1999.

[6] R. J. Gross and J. F. Osterle, "Membrane Transport Characteristics of Ultrafine Capillaries," *J. Chem. Phys.*, **49**, 228, 1968.

[7] S. Levin, J. R. Marriott, G. Neale, G. and N. Epstein, "Theory of Electrokinetic Flow in Fine Cylindrical Capillaries at High Zeta-Potentials" *J. Colloid Interface Sci.*, **52**, 136, 1975.